RESEARCH ARTICLE

Dimetal-Binding Scaffold 2-(Pyridin-2-yl)imidazo[1,5-*b*]pyridazine-7-ylidene: Synthesis of Trinuclear Heterobimetallic Complexes Involving Gold–Metal Interactions

Akito Kitabayashi,[b] Yuriko Ono,[a] Tetsuya Taketsugu,[a,b] Masaya Sawamura,*[a,b] Kosuke Higashida*[a]

[a] Dr. Y. Ono, Prof. Dr. T. Taketsugu, Prof. Dr. M. Sawamura, Dr. K. Higashida
Institute for Chemical Reaction Design and Discovery (WPI-ICReDD)
Hokkaido University
Kita 21 Nishi 10, Kita-ku, Sapporo 001-0021 (Japan)
E-mail: sawamura@sci.hokudai.ac.jp; higashida@icredd.hokudai.ac.jp

[b] A. Kitabayashi, Prof. Dr. T. Taketsugu, Prof. Dr. M. Sawamura
Department of Chemistry, Faculty of Science
Hokkaido University
Kita 10 Nishi 8, Kita-ku, Sapporo 060-0810 (Japan)

Abstract: As a dimetal-binding rigid scaffold, 2-(pyridin-2-yl)imidazo[1,5-*b*]pyridazine-7-ylidene was introduced. The scaffold was first converted into a meridional *Au*,*N*,*N*-tridentate ligand through binding of a Au(I)Cl moiety at the carbene center. The Au(I) center and the *N*,*N*-chelating moiety were expected to function as metallophilic and 4e-σ-donative interaction sites, respectively, in the binding of the second metal center. In this manner, various trinuclear heterobimetallic complexes were synthesized with different 3*d*-metal sources, such as cationic Cu^{I}, Cu^{II}, Ni^{II}, and Co^{II} salts. SC-XRD analysis showed that the mono-3*d*-metal di-gold(I) trinuclear heterobimetallic complexes were constructed through gold(I)-metal interactions. Metallophilic interactions were also investigated by quantum chemical calculations including the AIM and IGMH methods.

Introduction

N-Heterocyclic carbenes (NHCs) are recognized as soft metal coordinating ligands with strong σ-donating abilities, tightly binding various transition metals. Thus, NHC-ligated metal complexes have found wide application in catalysis, materials science, and medicinal chemistry.[1] Specifically, NHC-gold(I) complexes have been intensively studied for their catalytic activities as π-acids,[2] photophysical properties,[3] and bioactivities,[4] having the advantage of pronounced affinity between the gold and the NHC ligand to form a stable soft Lewis pair. Along this line, various gold(I)-containing heterobimetallic complexes[5] have been prepared with hybrid ligands containing an NHC site and another heteroatom-based σ-donor site such as an *N*-heteroaromatic for exploring metal-metal interactions.[6] In 2004, Catalano and co-workers utilized two types of pyridyl-substituted imidazolylidene ligands (Figure 1a) to prepare gold-silver complexes including gold(I)···silver(I) interactions.[7] Additionally, the related NHC-ligand systems were applied for constructing gold(I)-containing hetero-dimetal complexes,[8] in which the second metal was introduced by σ-donor coordination of multi-pyridine sites. To establish further reliable coordination of σ-donor sites to a metal atom, Roesky and co-workers introduced a bipyridine moiety with a methylene bridge to the NHC ligand (Figure 1b).[9] However, in some cases, the two metals were located away from each other, resulting in failure to achieve metal-metal interactions, probably due to the flexible nature of the methylene linker.[9,10]

Along this line, we envisioned that imidazo[1,5-*b*]pyridazine-7-ylidene, which has not been described in the literature,[11] would be a suitable molecular scaffold for synthesizing heterobimetallic complexes with a metal-metal interaction. In fact, we designed and synthesized 2-(pyridin-2-yl)imidazo[1,5-*b*]pyridazine-7-ylidene and converted it into the corresponding η^1-carbene-gold(I) complex. We expected the gold complex would act as a meridional *Au*,*N*,*N*-tridentate ligand for complexation of a second metal of the desired dimetal complex through providing metallophilic and *N*,*N*-4e-σ-donative interactions (Figure 1c,d). Specifically, we synthesized gold(I) chloride complex **1** and demonstrated its utility as a meridional *Au*,*N*,*N*-tridentate ligand in the preparation of various trinuclear heterobimetallic complexes with different 3*d*-metal species (Figure 1e). Metal-metal interactions in the trinuclear heterobimetallic complexes were confirmed by SC-XRD analysis and further analysed by quantum chemical calculations using the AIM and IGMH methods.

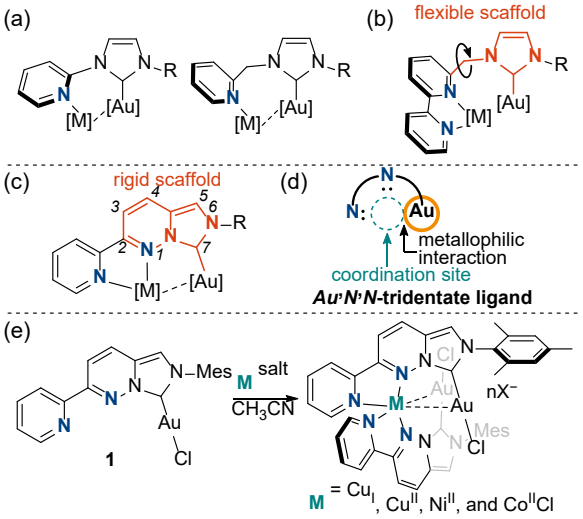

Figure 1. (a) Structures of reported NHC ligands including a pyridine coordination site, (b) structure of reported NHC ligands including a bipyridine coordination site, (c) structure of pyridyl-substituted imidazo[1,5-*b*]pyridazine-7-ylidene ligand, (d) our design strategy, and (e) this work.

Results and Discussion

The synthesis of 2-(pyridin-2-yl)imidazo[1,5-*b*]pyridazin-6-ium salt as a NHC precursor is shown in Figure 2. The methoxycarbonyl group of commercially available methyl 6-chloropyridazine-3-carboxylate (**2**) was converted into a formyl group through reduction with diisobutylaluminum hydride,[12] and the subsequent acetal protection gave **3** in 68% yield (over 2 steps). A 2-pyridyl group was introduced through palladium-catalysed cross-coupling between **3** and tributyl(2-pyridyl)tin. Acidic acetal deprotection afforded 6-(pyridin-2-yl)pyridazine-3-carbaldehyde (**4**) in 59% yield (over 2 steps). Next, three-component cyclization with **4**, 2,4,6-trimethylanilinium chloride, and paraformaldehyde gave NHC precursor **5** in 80% yield.[13] The reaction of **5** and AuCl·SMe_2 in the presence of K_2CO_3 in acetone furnished the NHC-gold(I) complex **1** in 65% yield.[14] SC-XRD analysis of a single crystal of **1** grown from DCM/Et_2O solution revealed that the gold complex adopts a linear two-coordinate geometry with the pyridyl coordination site uncoordinated as shown in Figure 2. The $C_{carbene}$–Au bond length is 1.976(2) Å, which is comparable to those for reported NHC-gold(I) chloride complexes.[15]

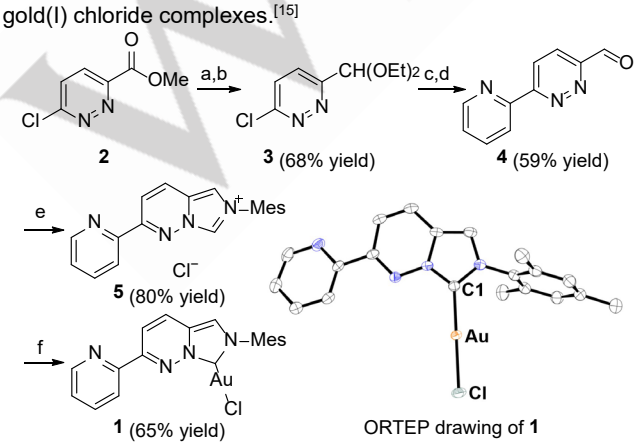

Figure 2. Procedure for the synthesis of gold complex **1**. a) **2** (1.0 equiv), DIBAL-H (1.2 equiv), toluene/THF, 0 °C, 20 min; b) $HC(OEt)_3$ (1.7 equiv), $TsOH·H_2O$ (5 mol%), EtOH, rt, 15 h; c) **3** (1.0 equiv), 2-pyridylSnBu_3 (1.0 equiv), $Pd(PPh_3)_4$ (6.7 mol%), toluene, 110 °C, 40 h; d) 1 M HCl aq/acetone (1/1), 60 °C, 3 h; e) **4** (1.0 equiv), paraformaldehyde (2.0 equiv), 2,4,6-trimethylanilinium chloride (1.5 equiv), EtOH, 30 °C, 16 h; f) **5** (1.0 equiv), AuCl·SMe_2 (1.0 equiv), K_2CO_3 (2.0 equiv), acetone, 60 °C, 3 h. Hydrogen atoms are omitted for clarity from the ORTEP drawing of **1** showing 50% probability thermal ellipsoids. Selected bond lengths [Å] and angle [deg] for **1**: C1–Au 1.976(2), Au–Cl 2.2791(6), C1–Au–Cl 178.16(7).[16]

With the gold(I) complex **1** in hand, a heterometallic complex was synthesized with a neutral copper(I) chloride salt (eq. 1). When **1** was treated with 1.0 equiv of CuCl in acetonitrile at room temperature, **1-Cu^{I}Cl** was obtained in 56% yield as purple plate crystals after recrystallization (CH_3CN/Et_2O). Single crystals of **1-Cu^{I}Cl** suitable for SC-XRD analysis were grown from a DCM/TBME solution. SC-XRD analysis disclosed that **1-Cu^{I}Cl** was a trinuclear complex containing a copper(I) cation and two gold(I) complexes with a non-coordinative $(CuCl_2)^-$ anion.

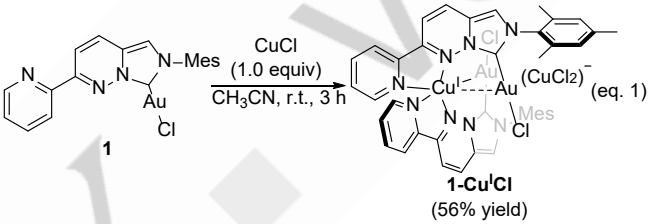

The result of complexation between **1** and CuCl, in which the copper atom was ionized upon coordination of the two bipyridine units, prompted us to use cationic copper(I) and copper(II) salts for constructing simpler trinuclear heterobimetallic complexes (Scheme 1). When 0.5 equiv of $[Cu(CH_3CN)_4]BF_4$ was mixed with **1** in acetonitrile at room temperature, **1-Cu^{I}** was obtained through recrystallization (CH_3CN/Et_2O) in 65% yield as thin-plate purple crystals. Single crystals of **1-Cu^{I}** suitable for structure determination were grown from an acetone/Et_2O solution. The trinuclear structure of **1-Cu^{I}** was unambiguously determined by SC-XRD analysis (Figure 3a) and found to be virtually the same as that of **1-Cu^{I}Cl**. Similarly, trinuclear heterobimetallic complex (**1-Cu^{II}**) bearing a copper(II) species was synthesized and isolated as plate brown crystals in 29% yield through the reaction between **1** and $Cu(NTf_2)_2$ followed by recrystallization (CH_3CN/TBME). The SC-XRD analysis showed that the molecular structure of **1-Cu^{II}** is nearly identical to that of **1-Cu^{I}** (Figure 3b).

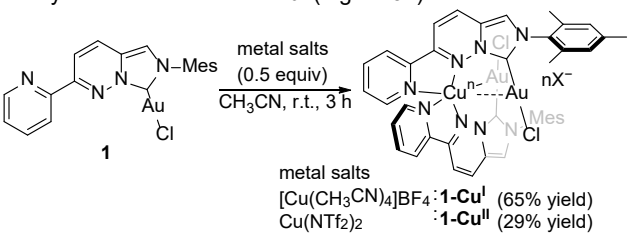

Scheme 1 Synthesis of copper-gold(I) heterobimetallic complexes.

The selected bond lengths and angles for **1-Cu^{I}** and **1-Cu^{II}** are given in Table 1. The trinuclear cores of these heterobimetallic complexes consist of one copper atom and two gold(I) atoms. The copper centers adopt distorted octahedral geometries with meridional *Au,N,N*-tridentate coordination of two molecules of gold(I) complex **1**. The Cu–Au distances for **1-Cu^{I}** are 3.0820(6)

and 3.0223(6) Å, which are slightly longer and shorter, respectively, than the sum of their van der Waals radii (3.06 Å).[17] Such Cu–Au lengths are longer than those for reported trinuclear copper(I)-gold(I) heterometallic complexes **6**, **7**, and **8** with two 2-(diphenylphosphino)pyridine (PPh_2py) ligands (Figure 4).[18-20] These variations of Cu–Au bond lengths between **1-Cu^{I}** and **6**-**8** may correspond to the difference in the number of valence electrons of the copper(I) centers. While the d^{10} copper(I) center of **1-Cu^{I}**, which is coordinated with the four *N*-σ-donor ligands, has eighteen valence electrons, those of **6**-**8** with the two *N*-σ-donor ligands have only fourteen electrons. On the other hand, the Cu–Au distances [2.8338(5) and 2.8212(5) Å] of **1-Cu^{II}** are clearly shorter than those of **1-Cu^{I}**, indicating that intermetallic interactions of **1-Cu^{II}** are stronger than those of **1-Cu^{I}**. The fewer number of valence electrons for **1-Cu^{II}** than that for **1-Cu^{I}** may be the cause of the stronger interactions in **1-Cu^{II}**. Additionally, the N3–Cu–N7 angle for **1-Cu^{I}** is bent to 156°, resulting in a highly distorted octahedral geometry of **1-Cu^{I}**, whereas the N3–Cu–N7 angle (174°) for **1-Cu^{II}** is almost 180°, giving only a slightly distorted octahedral geometry for **1-Cu^{II}**. The coordination geometry of **1-Cu^{II}** resembles that of reported [Cu(II)(*mer*-terpyridine)$_2$]$^{2+}$-type complexes,[21] while copper(I) species generally prefer a lower coordination number as in four-coordinate tetrahedral complexes.[22] Considering these intrinsic coordination tendencies of copper complexes, the higher tolerance of the Cu(II) center for accepting an octahedral geometry may be the cause of the stronger Au···Cu interactions of **1-Cu^{II}**.

Table 1. Selected Bond Lengths [Å] and Angles [deg] for **1-Cu^{I}** and **1-Cu^{II}**

	1-Cu^{I}	**1-Cu^{II}**
Cu–Au1	3.0820(6)	2.8338(5)
Cu–Au2	3.0223(6)	2.8212(5)
Au1–Au2	3.46079(18)	3.43764(17)
Cu–N3	1.983(4)	1.950(3)
Cu–N4	2.077(4)	2.092(3)
Cu-N7	1.986(3)	1.956(3)
Cu–N8	2.043(4)	2.093(3)
Au1–Cu–Au2	69.067(12)	74.875(13)
N3–Cu–N7	156.17(15)	174.14(13)
N3–Cu–N4	79.20(15)	78.75(13)
N7–Cu–N8	79.04(14)	78.80(12)

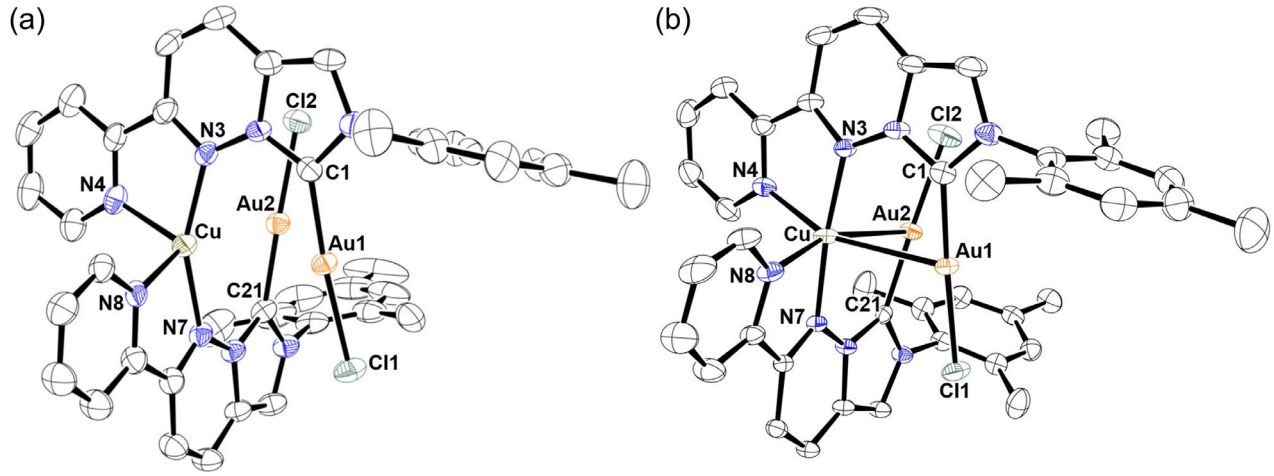

Figure 3. ORTEP drawings of (a) **1-Cu^{I}** and (b) **1-Cu^{II}**. All hydrogen atoms, counter anions, and solvent molecules are omitted for clarity from the ORTEP drawings showing 50% probability thermal ellipsoids.[16]

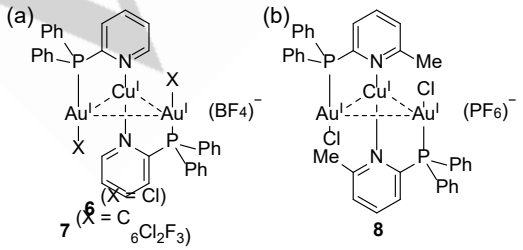

Figure 4. Structures of reported trinuclear copper(I)-gold(I) complexes. (a) Cu–Au distances for $[Au_2CuCl_2(PPh_2py)_2]BF_4$ (**6**: X = Cl) are 2.9827(11) and 3.0485(11) Å.[18] Cu–Au distances for $[Au_2Cu(C_6Cl_2F_3)_2(PPh_2py)_2]BF_4$ (**7**: X = $C_6Cl_2F_3$) are 2.9647(6) and 2.8403(5) Å.[19] (b) Cu–Au distances for $[Au_2CuCl_2(PPh_2\text{-}6\text{-}Mepy)_2]PF_6$ (**8**) are 2.8087(5) and 2.8374(5) Å.[20]

Next, to examine d^8-d^{10} and d^7-d^{10} metal-metal interactions with gold(I) complex **1**, heterometallic complexes were prepared using cationic nickel(II) and cobalt(II) salts (Scheme 2). When complex **1** was treated with $[Ni(H_2O)_6](BF_4)_2$, **1-Ni^{II}** was obtained through recrystallization (CH_3CN/Et_2O) in 71% yield as fine yellow crystals. Further recrystallization from a DCM/benzene solution gave single crystals of **1-Ni^{II}** suitable for structure determination. SC-XRD analysis revealed that **1-Ni^{II}** has a trinuclear structure

similar to those of the copper-gold(I) complexes (Figure 5a). A cobalt(II)-gold(I) heterobimetallic complex was synthesized from complex **1**, in which $Co(NTf_2)_2$ was utilized as a cationic cobalt(II) salt. After mixing **1** and 0.5 equiv of $Co(NTf_2)_2$ in acetonitrile, recrystallization (CH_3CN/Et_2O) gave **1-Co^{II}Cl** as yellow crystalline needles in 57% yield. SC-XRD analysis of a yellow crystal disclosed the trinuclear structure of **1-Co^{II}Cl**; however, a chloride ligand was bonded to the cobalt(II) metal center (Figure 5b). The chloride ligand of the cobalt complex could possibly have originated from gold complex **1** through decomposition to form cationic bis-NHC-gold complexes, as discussed later.

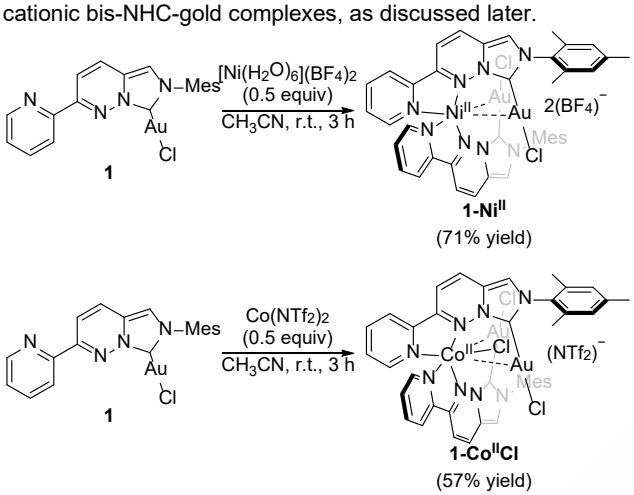

Scheme 2 Synthesis of nickel(II)- and cobalt(II)-gold(I) heterobimetallic complexes.

Selected bond lengths and angles for **1-Ni^{II}** and **1-Co^{II}Cl** are given in Table 2. In the **1-Ni^{II}** complex, the nickel center has an octahedral geometry with two meridional *Au*,*N*,*N*-tridentate ligands. Ni–Au contacts [2.7810(5) and 2.8083(5) Å] for **1-Ni^{II}** are much shorter than the sum of their van der Waals radii (3.29 Å),[17] indicating that nickel(II)–gold(I) contacts in **1-Ni^{II}** have intermetallic interactions. The N3–Ni–N7 bond for **1-Ni^{II}** is almost linear (176°), as in the **1-Cu^{II}** complex, leading to a slightly distorted octahedral environment for the nickel center. The cobalt center of **1-Co^{II}Cl** has an apparent pentagonal bipyramidal coordination environment with two axial $N_{pyridazine}$ ligands, two equatorial $N_{pyridyl}$ ligands, two equatorial gold atoms, and an equatorial chloride ligand. The axial N–Co–N bond is nearly linear [171.88(9)°]. The equatorial bond angle of N–Co–N [93.59(9)°] is larger than those of N–Co–Au [70.46(7) and 72.45(7)°] and Au–Co–Cl [69.62(2) and 68.83(2)°], adopting a distorted pentagonal structure. The Co–Au distances [3.2086(5) and 3.2838(5) Å] are slightly shorter than the sum of the van der Waals radii of Co and Au,[23] indicating the presence of intermetallic interactions between a cobalt(II) atom and gold(I) atoms.

Table 2. Selected Bond Lengths [Å] and Angles [deg] for **1-Ni^{II}** and **1-Co^{II}Cl**

1-Ni^{II}			
Ni–Au1	2.7810(5)	Ni–N8	2.046(3)
Ni–Au2	2.8083(5)	Au1–Ni–Au2	77.592(13)
Au1–Au2	3.5021(2)	N3–Ni–N7	175.82(13)
Ni–N3	1.985(3)	N3–Ni–N4	78.64(13)
Ni–N4	2.033(3)	N7–Ni–N8	78.61(13)
Ni–N7	1.986(3)		
1-Co^{II}Cl			
Co–Au1	3.2086(5)	N3–Co–N7	171.88(9)
Co–Au2	3.2838(5)	N4–Co–N8	93.59(9)
Co–N3	2.149(2)	N4–Co–Au2	70.46(7)
Co–N4	2.076(2)	N8–Co–Au1	72.45(7)
Co–N7	2.163(2)	Au1–Co–Cl3	69.62(2)
Co–N8	2.067(2)	Au2–Co–Cl3	68.83(2)
Co–Cl3	2.2775(8)	N3–Co–N4	76.00(9)
Au1–Co–Au2	138.165(12)	N7–Co–N8	75.98(9)

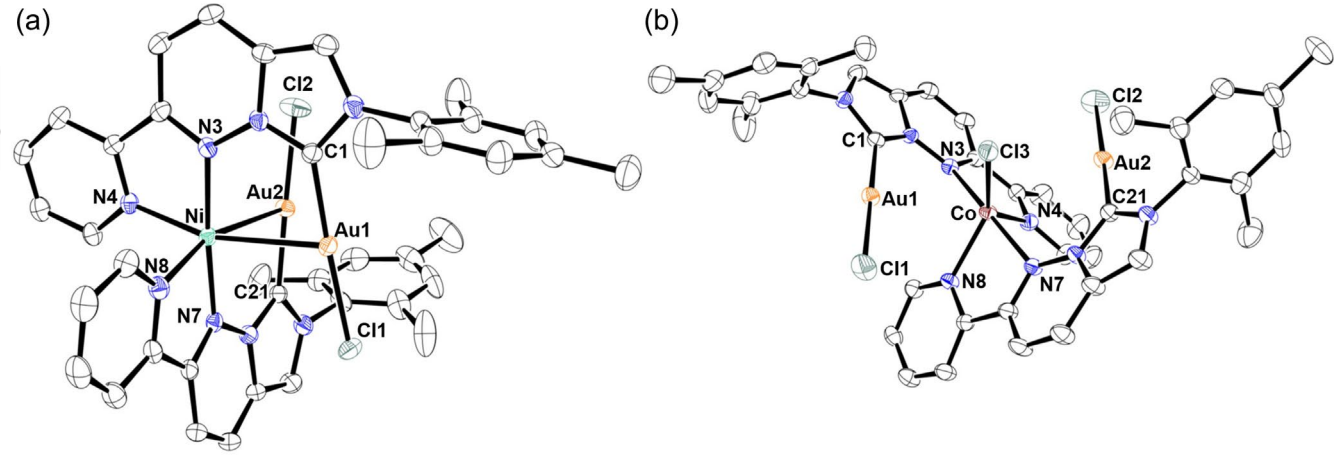

Figure 5. ORTEP drawings of (a) **1-Ni^{II}** and (b) **1-Co^{II}Cl**. All hydrogen atoms, counter anions, and solvent molecules are omitted for clarity from the ORTEP drawings showing 50% probability thermal ellipsoids.[16]

When we attempted to synthesize d^6-d^{10} heterobimetallic complexes with a cationic iron(II) salt by the use of **1** and $[Fe(H_2O)_6](BF_4)_2$ in acetonitrile, light-yellow crystals as well as reddish brown precipitates were obtained after recrystallization (CH_3CN/Et_2O) (see Supporting Information). SC-XRD analysis of the light-yellow crystal revealed that gold complex **1** decomposed to bis-NHC-gold(I) cationic complex **9** (Figure 6a). This result indicates that the chloride ligand bonded to the cobalt atom of **1-Co^{II}Cl** might be supplied through such decomposition forming a cationic bis-NHC-gold(I) complex. The bis-NHC-gold(I) complex **10** was also obtained in 47% yield from the reaction of **1** and 0.75 equiv of $[Fe(H_2O)_6](BF_4)_2$ after quenching with *N*,*N*-diisopropylethylamine followed by sequential purification through silica-gel column chromatography and basic-alumina column chromatography (Figure 6b). Further attempts to obtain crystal structures of iron(II)-gold(I) heterobimetallic complexes were unsuccessful.

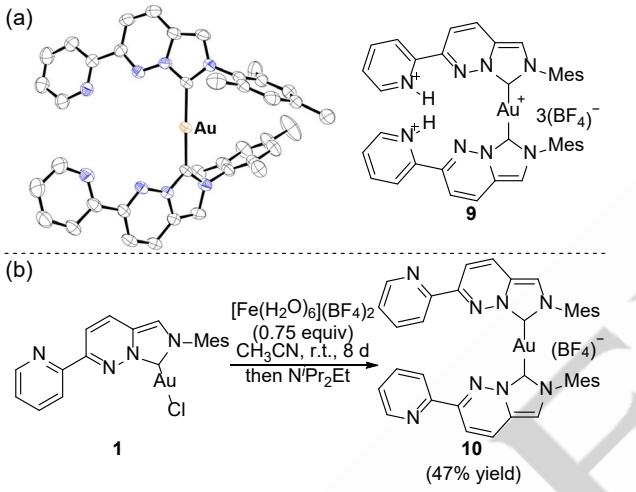

Figure 6. (a) An ORTEP drawing of **9**. All hydrogen atoms, counter anions, and solvent molecules are omitted for clarity from the ORTEP drawing showing 50% probability thermal ellipsoids. (b) Synthesis of cationic bis-NHC-gold(I) complex **10**.[16]

Emission properties of **1-Cu^{I}**, **1-Ni^{II}**, and **1-Co^{II}Cl** were assessed. Consequently, **1-Cu^{I}** is not luminescent in dichloromethane, whereas gold complex **1** showed blue emission centered at 457 nm (exc. 360 nm) in dichloromethane at room temperature. Solutions of **1-Ni^{II}** and **1-Co^{II}Cl** in dichloromethane showed emissions centered at 455 nm and 459 nm (exc. 360 nm), respectively. Since their emission spectra are almost identical in shape with that of gold complex **1**, these emissions might be attributable to the dissociated gold complex **1** in the solution. Instability of **1-Cu^{II}** in a solution phase hampered the measurement of a luminescent spectrum for **1-Cu^{II}**.

Properties of interactions in the trinuclear heterobimetallic complexes were investigated by quantum chemical calculations. Molecular structures of trinuclear heterobimetallic complexes obtained from SC-XRD analysis were fully optimized as monocationic species or dicationic species without non-coordinative counter anions at the ωB97X-D/def2tzvp level of theory using the Gaussian 16 C.01 package.[24] **1-Ni^{II}** and **1-Co^{II}Cl** were calculated in the lowest energy spin states, triplet and quartet spin states, respectively. In the optimized structures, whereas Cu–Au interatomic distances (3.12 and 3.12 Å) for **1-Cu^{I}** are slightly longer than the bond lengths (3.02 and 3.08 Å) for **1-Cu^{I}** indicated by the SC-XRD analysis, Cu–Au interatomic distances (2.82 and 2.82 Å) for **1-Cu^{II}** are in accord with the experimental observations (2.82 and 2.83 Å). The nickel(II)-gold(I) interatomic distances (2.80 and 2.80 Å) for optimized structures of **1-Ni^{II}** agree well with the crystallographic data (2.78 and 2.81 Å). However, cobalt(II)–gold(I) interatomic distances (3.38 and 3.42 Å) for the optimized structures of **1-Co^{II}Cl** are about 0.15 Å longer than those from the crystallographic data (3.21 and 3.28 Å). To elucidate the properties of 3*d*-metal–gold(I) heterointeractions, an Atoms In Molecules (AIM) analysis[25] was performed for the optimized structures using the Multiwfn program,[26,27] as shown in Figure 7. In **1-Cu^{I}**, bond critical points (BCPs) were observed not only for the copper(I)···gold(I) contacts but also for the gold(I)···gold(I) contact. In contrast, **1-Cu^{II}** had no BCP for the gold(I)···gold(I) contact, indicating that the valence of copper clearly impacts the behavior of metallophilic interactions over the trinuclear metal complexes. While such a gold(I)···gold(I) contact was also absent in **1-Ni^{II}**, BCPs were observed for the nickel(II)···gold(I) contacts. A BCP existed only for one of the two cobalt(II)···gold(I) contacts in **1-Co^{II}Cl**. For all of the trinuclear heterobimetallic complexes, the calculated values for electron density ρ and positive values for the Laplacian of the electron density $\Delta\rho$ at the BCPs indicated that these 3*d*-metal···gold(I) contacts are characterized as metallophilic interactions. The noncovalent characters of these 3*d*-metal–gold(I) bonds were also indicated by the small values of the electron localization function (ELF)[28] at the BCPs, as shown in Figure 7. In addition, these ρ values indicate that the copper(I)···gold(I) interactions of **1-Cu^{I}** are clearly weaker than the copper(II)···gold(I) interactions of **1-Cu^{II}**, while the strength of d^8-d^{10} metal-metal interactions of **1-Ni^{II}** are similar to those of d^9-d^{10} metal-metal interactions of **1-Cu^{II}**. The metallophilic interaction of cobalt(II)···gold(I) of **1-Co^{II}Cl** is much weaker than those of **1-Cu^{I}**, **1-Cu^{II}**, and **1-Ni^{II}**. Metallophilic interactions of **1-Cu^{I}**, **1-Cu^{II}**, **1-Ni^{II}**, and **1-Co^{II}Cl** were visualized through the independent gradient model based on the Hirshfeld partition (IGMH) method[29] in the Multiwfn program[26] as shown in Figure 8. Two fragments for IGMH were defined as two gold atoms and a 3*d*-metal atom for clarifying the visualization. Weak attractive interactions were clearly found between 3*d*-metal and gold atoms, in which interactions over **1-Cu^{II}** and **1-Ni^{II}**, shown as greenish blue, were stronger than those of **1-Cu^{I}** shown in green. In **1-Co^{II}Cl**, small green regions were found for both the cobalt(II)···gold(I) contacts, indicating that noncovalent interactions between cobalt(II) and gold(I) atoms are weak.

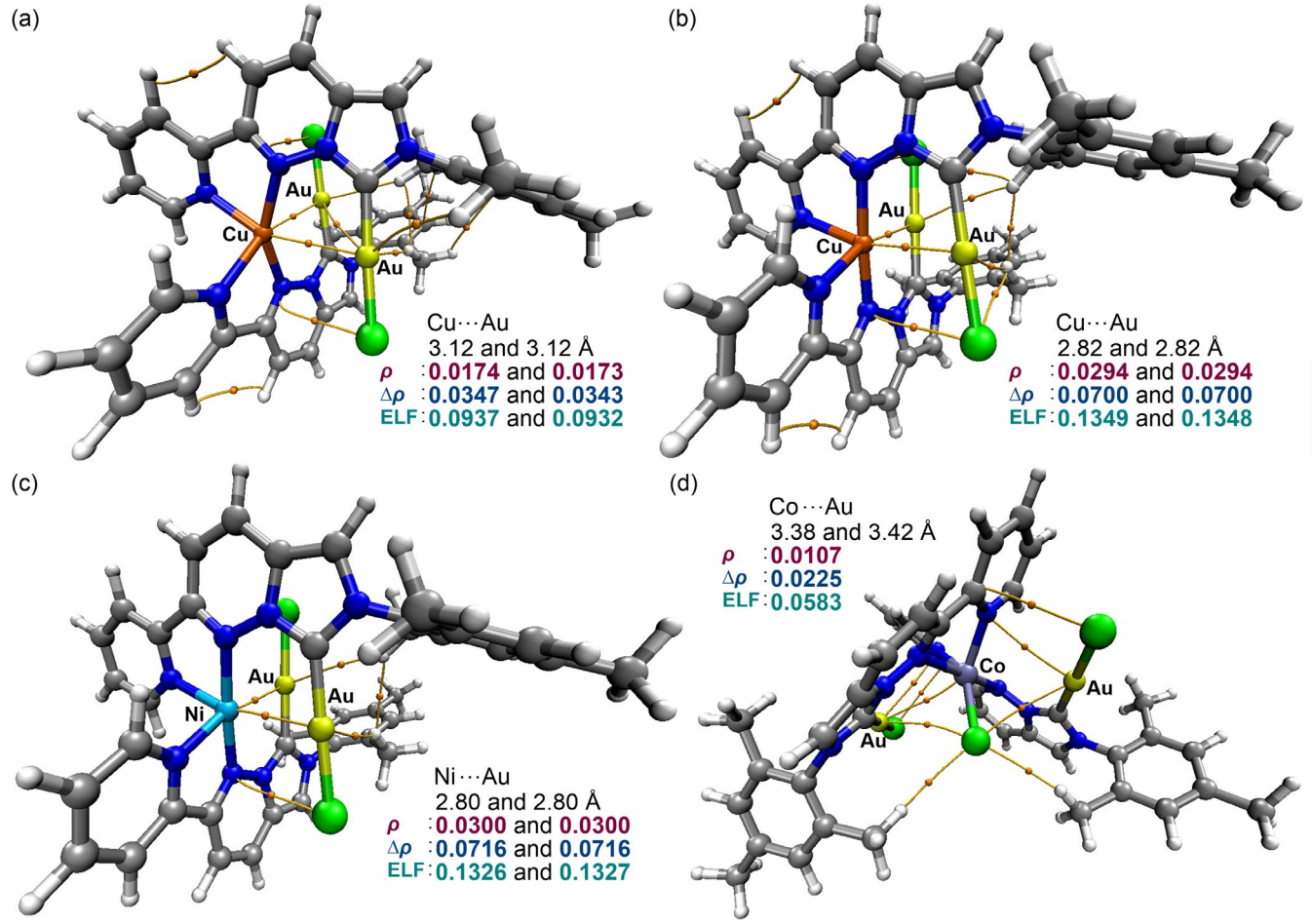

Figure 7. Molecular structures for (a) **1-Cu^{I}**, (b) **1-Cu^{II}**, (c) **1-Ni^{II}**, and (d) **1-Co^{II}Cl**. Bond critical points (orange) are shown in molecular structures. Bond lengths (black) and electron density (red), Laplacian of electron density (blue), and values of ELF (green) at the BCPs of two 3d-metal···gold(I) contacts are given.

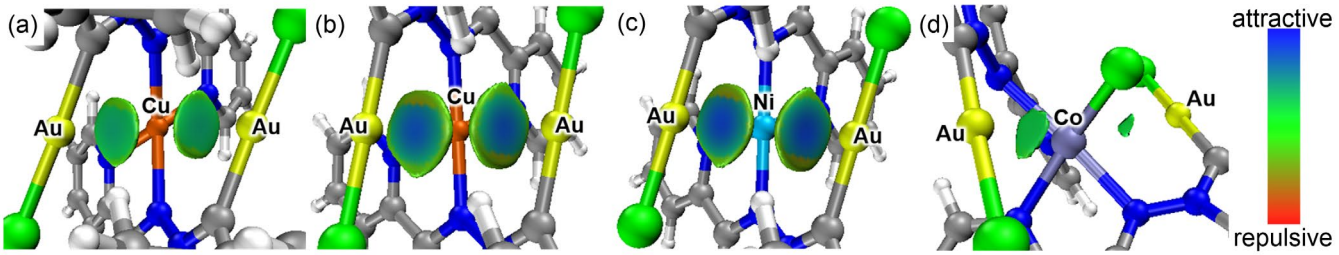

Figure 8. IGMH for (a) **1-Cu^{I}**, (b) **1-Cu^{II}**, (c) **1-Ni^{II}**, and (d) **1-Co^{II}Cl** mapped with coloured isosurfaces for δg^{inter} = 0.010 a.u. The color scale for the mapped function sign(λ_2)ρ is –0.05 < sign(λ_2)ρ < 0.05.

Conclusion

An imidazo[1,5-*b*]pyridazine-7-ylidene scaffold and an *Au*,*N*,*N*-tridentate ligation strategy have been introduced for the synthesis of hetero-dimetal complexes with gold(I)-metal intermetallic interactions. Gold(I)-3*d*-metal trinuclear heterobimetallic complexes **1-Cu^{I}**, **1-Cu^{II}**, **1-Ni^{II}**, and **1-Co^{II}Cl** were prepared through complexation of 3*d*-metal salts with an *Au*,*N*,*N*-tridentate ligand **1**, which is composed of metallophilic gold(I) and *N*,*N*'-4e-σ-donor ligand moieties. The detailed molecular structures of the trinuclear heterobimetallic complexes were determined by SC-XRD analysis, and the results indicated that metallophilic interactions exist between the gold(I) and the 3*d*-metals. The metallophilic interactions were also supported by the AIM and IGMH analyses.

Experimental Section

Synthesis of 3-Chloro-6-(diethoxymethyl)pyridazine (3): Methyl 6-chloropyridazine-3-carboxylate (5.17 g, 30.0 mmol) was added to dry THF (130 mL) under nitrogen atmosphere, and the

suspension was cooled at 0 °C. Diisobutylaluminum hydride solution (1M in toluene, 36.0 mL, 36.0 mmol, 1.2 equiv) was added dropwise to the mixture over 10 minutes, and the reaction mixture was stirred at 0 °C for 20 minutes. After quenching the mixture with 1M HCl aqueous solution, the reaction mixture was neutralized with saturated $NaHCO_3$ aqueous solution at room temperature. An excess amount of Rochelle salt was added to the mixture, and the resulting white suspension was vigorously stirred for 4 hours. The aqueous layer was extracted with EtOAc and DCM, and the combined organic layer was dried over Na_2SO_4, filtrated, and evaporated. The crude mixture was passed through silica-gel with an eluent (EtOAc/hexane = 1/3 to 1/2) to remove high polar impurities. The resulting brown oil was placed in a Schlenk tube and dissolved in EtOH (15 mL) under nitrogen atmosphere. $TsOH \cdot H_2O$ (286 mg, 1.5 mmol, 5.0 mol %) and triethyl orthoformate (8.23 mL, 50 mmol, 1.7 equiv) were added to the mixture, and the resulting solution was stirred for 15 hours. The mixture was quenched with saturated $NaHCO_3$ aqueous solution and extracted with EtOAc. The combined organic layer was dried over Na_2SO_4, filtrated, and evaporated. A residue was purified by silica-gel column chromatography (hexane to EtOAc/hexane = 1/4) to afford the desired product (4.45 g, 20.5 mmol, 68% yield).

White solid. M.p.: 31-33 °C. IR (ATR, ν/cm^{-1}): 2976 m, 2930 w, 2879 w, 1569 w, 1542 w, 1481 w, 1444 w, 1413 w, 1369 w, 1319 m, 1136 m, 1108 s, 1059 s, 914 m, 839 m, 658 w. ^{1}H NMR (400 MHz, $CDCl_3$, 25 °C): δ 7.74 (d, *J* = 8.9 Hz, 1H), 7.55 (dd, *J* =8.9, 0.5 Hz, 1H), 5.66 (s, 1H), 3.84-3.75 (m, 2H), 3.67-3.58 (m, 2H), 1.25 (t, *J* = 7.1 Hz, 6H). ^{13}C{^{1}H} NMR (100 MHz, $CDCl_3$, 25 °C): δ 160.1, 157.0, 129.0, 127.1, 101.6, 63.4, 15.1. HRMS (ESI$^+$) m/z calc. for $C_9H_{13}N_2O_2ClNa$ 239.0558 found 239.0557.

Synthesis of 6-(Pyridin-2-yl)pyridazine-3-carbaldehyde (4): 3-Chloro-6-(diethoxymethyl)pyridazine (1.08 g, 5.0 mmol) was placed in a Schlenk tube, and the Schlenk tube was introduced in an argon-filled glove box. After addition of $Pd(PPh_3)_4$ (390 mg, 0.34 mmol, 6.7 mol%), the solid compounds were dissolved in dry toluene (25 mL). Tributyl(2-pyridyl)tin (1.6 mL, 5.0 mmol, 1.0 equiv) was added to the mixture, and the Schlenk tube was taken out from the glove box. The mixture was heated at 110 °C for 40 hours and filtered through 10 wt% K_2CO_3 on silica-gel with EtOAc as an eluent, and volatiles were removed under reduced pressure. A residue was purified by 10 wt% K_2CO_3 on silica-gel column chromatography (EtOAc/hexane = 1/4) to give the yellow solid. The solid compound was dissolved in acetone (20 mL) and 1M HCl aqueous solution (20 mL), and a mixture was heated at 60 °C for 3 hours. The resulting mixture was quenched by $NaHCO_3$ aqueous solution, and extracted with DCM. The organic layer was dried over Na_2SO_4, filtrated, and evaporated. A residue was purified by silica-gel column chromatography (EtOAc/hexane = 1/4 to 1/2) to afford the desired product (546 mg, 2.95 mmol, 59% yield).

Yellow solid. M.p.: 156-158 °C. IR (ATR, ν /cm^{-1}): 3065 w, 2832 w, 2397 w, 1710 m, 1585 w, 1567 m, 1548 m, 1470 w, 1434 w, 1412 m, 1351 m, 1276 m, 1210 m, 1141 m, 1113 m, 1057 m, 1036 m, 1021 w, 990 m, 859 m, 835 m, 797 s, 754 s, 743 s, 674 m, 643 m, 614 m, 567 m, 511 m. ^{1}H NMR (400 MHz, $CDCl_3$, 25 °C): δ 10.46 (d, *J* = 0.9 Hz, 1H), 8.82-8.74 (m, 3H), 8.16 (d, *J* = 8.9 Hz, 1H), 7.94 (td, *J* = 7.8, 1.8 Hz, 1H), 7.46 (ddd, *J* = 7.6, 4.7, 1.2 Hz, 1H). ^{13}C{^{1}H} NMR (100 MHz, $CDCl_3$, 25 °C): δ 192.1, 160.4, 155.0, 152.4, 149.8, 137.4, 125.6, 125.3, 124.9, 122.7. HRMS (ESI$^+$) m/z calc. for $C_{10}H_7ON_3Na$ 208.0481 found 208.0480.

Synthesis of 2-(2-Pyridyl)-6-mesitylimidazo[1,5-*b*]pridazin-6-ium Chloride (5): 6-(Pyridin-2-yl)pyridazine-3-carbaldehyde (185 mg, 1.0 mmol), 2,4,6-trimethylaniline hydrochloride (258 mg, 1.5 mmol, 1.5 equiv), and paraformaldehyde (60.4 mg, 2.0 mmol, 2.0 equiv) were dissolved in EtOH (5.0 mL). After stirring at 30 °C for 16 hours, all volatile compounds were removed under reduced pressure. A residue was purified by silica-gel column chromatography (DCM/MeOH = 9/1 to 4/1) followed by basic alumina column chromatography (DCM to DCM/MeOH = 4/1) to afford the desired product (282 mg, 0.80 mmol, 80% yield).

Pale brown solid. M.p.: 133 °C (decomp.). IR (ATR, /cm^{-1}): 3378 w, 3033 m, 2951 m, 2919 m, 2735 w, 1636 m, 1606 w, 1585 m, 1567 m, 1521 w, 1495 m, 1463 m, 1436 m, 1414 m, 1383 m, 1337 w, 1323 m, 1283 m, 1235 m, 1195 m, 1152 m, 1095 w, 1061 m, 1038 m, 994 m, 950 w, 852 m, 786 m, 726 s, 696 m, 675 m, 647 m, 633 m, 617 m, 585 m, 553 m. ^{1}H NMR (400 MHz, $CDCl_3$, 25 °C): δ 10.53 (d, *J* = 1.8 Hz, 1H), 9.03 (d, *J* = 9.6 Hz, 1H), 8.81-8.76 (m, 2H), 8.51 (d, *J* = 7.8 Hz, 1H), 8.34 (d, *J* = 9.6 Hz, 1H), 7.91 (td, *J* = 7.8, 1.8 Hz, 1H), 7.51 (ddd, *J* = 7.6, 4.8, 0.9 Hz, 1H), 7.04 (s, 2H), 2.36 (s, 3H), 2.10 (s, 6H). ^{13}C{^{1}H} NMR (100 MHz, $CDCl_3$, 25 °C): δ 157.8, 150.0, 149.7, 141.8, 137.5, 134.0, 131.1, 130.0, 129.5, 129.3, 126.5, 125.9, 122.7, 117.53, 117.50, 21.2, 17.7. HRMS (ESI$^+$) m/z calc. for $C_{20}H_{19}N_4$ 315.1604 found 315.1603.

Synthesis of Gold(I) Complex (1): In a nitrogen-filled grove box, dry acetone (3.0 mL) was added to the 2-(2-pyridyl)-6-mesitylimidazo[1,5-*b*]pridazin-6-ium chloride (105 mg, 0.30 mmol), K_2CO_3 (82.9 mg, 0.60 mmol, 2.0 equiv) and $AuCl \cdot SMe_2$ (88.8 mg, 0.30 mmol, 1.0 equiv) placed in a screw-cap vial. The vial was sealed with a screw-cap and taken out from the glove box. After stirring at 60 °C for 3 hours under dark conditions, the mixture was passed through a celite pad to remove insoluble materials. Volatiles were removed under reduced pressure, and a residue was purified by silica-gel column chromatography (only DCM) to afford the product (106 mg, 0.194 mmol, 65% yield).

Pale yellow solid. M.p.: 120 °C (decomp.). IR (ATR, ν/cm^{-1}): 3132 w, 3036 w, 2918 w, 1639 w, 1584 w, 1567 w, 1493 m, 1462 m, 1439 w, 1415 w, 1364 w, 1340 m, 1301 m, 1283 w, 1267 w, 1245 w, 1223 w, 1193 m, 1155 w, 1120 w, 1092 w, 1057 w, 1035 m, 997 w, 850 m, 830 m, 814 w, 789 s, 757 m, 736 m, 714 m, 703 m, 685 m, 655 w, 641 w, 617 w, 599 m, 578 w, 530 w. ^{1}H NMR (400 MHz, $CDCl_3$, 25 °C): δ 8.73 (ddd, *J* = 4.8, 1.6, 0.9 Hz, 1H), 8.62 (dt, *J* = 8.0, 1.0 Hz, 1H), 8.13 (d, *J* = 9.6 Hz, 1H), 7.95-7.88 (m, 2H), 7.46 (ddd, *J* = 7.5, 4.9, 1.1 Hz, 1H), 7.26 (s, 1H), 7.02 (s, 2H), 2.37 (s, 3H), 2.04 (s, 6H). ^{13}C{^{1}H} NMR (100 MHz, $CDCl_3$, 25 °C): δ 168.4 ($C_{carbene}$), 154.5, 151.3, 149.2, 140.2, 137.4, 135.3, 134.3, 129.6, 126.0, 125.7, 124.7, 122.4, 116.2, 112.4, 21.2, 17.9. HRMS (ESI$^+$) m/z calc. for $C_{20}H_{18}N_4AuClNa$ 569.0778 found 569.0785. UV-Vis absorption: λ [nm](ε [M^{-1}cm^{-1}]) in DCM: 279 (26145), 358 (1609). Emission (λ_{ex} = 360nm): λ [nm] in DCM: 457.

Supporting Information

Experimental details, SC-XRD analysis, computational data, and spectral data. Additional references cited within the Supporting Information.[30-34]

Acknowledgements

This work was supported by JSPS KAKENHI Grant No. JP20K15268 and JP23K13735 in Grant-in-Aid for Young Scientists to K.H. and Grant No. JP21H04680 in Grant-in-Aid for Scientific Research (A) to M.S.

Keywords: heterobimetallic complex • metallophilic interaction • *N*-heterocyclic carbene • gold complex • DFT calculation

[1] a) S. P. Nolan in N-Heterocyclic Carbenes, Wiley-VCH, **2014**; b) W. A. Herrmann, C. Köcher, *Angew. Chem., Int. Ed.* **1997**, *36*, 2162–2187; c) C. M. Crudden, D. P. Allen, *Coord. Chem. Rev.* **2004**, *248*, 2247–2273; d) O. Kühl, *Chem. Soc. Rev.* **2007**, *36*, 592–607; e) F. E. Hahn, M. C. Jahnke, *Angew. Chem., Int. Ed.* **2008**, *47*, 3122–3172; f) L. Oehninger, R. Rubbiani, I. Ott, *Dalton Trans.* **2013**, *42*, 3269–3284; g) M. H. Hopkinson, C. Richter, M. Schedler, F. Glorius, *Nature* **2014**, *510*, 485–496.

[2] a) N. Marion, S. P. Nolan, *Chem. Soc. Rev.* **2008**, *37*, 1776–1782; b) A. Mariconda, M. Sirignano, R. Troiano, S. Russo, P. Longo, *Catalysts* **2022**, *12*, 836.

[3] H. Amouri, *Chem. Rev.* **2023**, *123*, 230–270.

[4] S. Nayak, S. L. Gaonkar, *ChemMedChem* **2021**, *16*, 1360–1390.

[5] Selected examples, a) V. K. Rawat, K. Higashida, M. Sawamura, *ACS Catal.* **2022**, *12*, 8325–8330; b) A. Luengo, I. Marzo, V. Fernández-Moreira, M. C. Gimeno, *Appl. Organomet. Chem.* **2022**, e6661; c) Q. Teng, H. V. Huynh, *Organometallics* **2018**, *37*, 4119–4127; d) M. R. D. Gatus, M. Bhadbhade, B. A. Messerle, *Dalton. Trans.* **2017**, *46*, 14406–14419; e) Q. Teng, H. V. Huynh, *Chem. Commun.* **2015**, *51*, 1248–1251; f) B. Bertrand, A. Citta, I. L. Franken, M. Picquet, A. Folda, V. Scalcon, M. P. Rigobello, P. L. Gendre, A. Casini, E. Bodio, *J. Biol. Inorg. Chem.* **2015**, *20*, 1005–1020; g) L. Boselli, M. Carraz, S. Mazères, L. Paloque, G. González, F. Benoit-Vical, A. Valentin, C. Hemmert, H. Gornitzka, *Organometallics* **2015**, *34*, 1046–1055.

[6] a) M. Baradají, A. Laguna, *Eur. J. Inorg. Chem.* **2003**, 3069–3079; b) E. J. Fernández, A. Laguna, J. M. López-de-Luzuriaga, M. Monge, M. Montiel, M. E. Olmos, *Inorg. Chem.* **2007**, *46*, 2953–2955; c) E. J. Fernández, A. Laguna, J. M. López-de-Luzuriaga, *Dalton Trans.* **2007**, 1969–1981; d) M. Rodríguez-Castillo, M. Monge, J. M. López-de-Luzuriaga, M. E. Olmos, A. Laguna, F. Mendizabal, *Comp. Theor. Chem.* **2011**, *965*, 163–167; Au–Au interactions have also been investigated, e) H. Scbmidbaur, *Gold Bull.* **1990**, *23*, 11–21; f) H. Scbmidbaur, A. Schier, *Chem. Soc. Rev.* **2012**, *41*, 370–412.

[7] a) V. J. Catalano, M. A. Malwitz, A. O. Etogo, *Inorg. Chem.* **2004**, *43*, 5714–5724; b) V. J. Catalano, A. O. Etogo, *J. Organomet. Chem.* **2005**, *690*, 6041–6050; c) V. J. Catalano, A. L. Moore, *Inorg. Chem.* **2005**, *44*, 6558–6566; d) V. J. Catalano, A. O. Etogo, *Inorg. Chem.* **2007**, *46*, 5608–5615.

[8] a) V. J. Catalano, A. L. Moore, J. Shearer, J. Kim, *Inorg. Chem.* **2009**, *48*, 11362–11375; b) C. E. Strasser, V. J. Catalano, *Inorg. Chem.* **2011**, *50*, 11228–11234; c) M. M. Nenzel, K. Chen, V. J. Catalano, *J. Coord. Chem.* **2016**, *69*, 160–167; d) B. M. Kariuki, J. A. Platts, P. D. Newman, *RSC Adv.* **2021**, *11*, 34170–34173; e) V. R. Naina, F. Krätschmer, P. W. Roesky, *Chem. Commun.* **2022**, *58*, 5332–5346.

[9] a) C. Kaub, S. Lebedkin, S. Bestgen, R. Köppe, M. M. Kappes, P. W. Roesky, *Chem. Commun.* **2017**, *53*, 9578–9581; b) C. Kaub, S. Lebedkin, A. Li, S. V. Kruppa, P. H. Strebert, M. M. Kappes, C. Riehn, P. W. Roesky, *Chem. Eur. J.* **2018**, *24*, 6094–6104.

[10] Other flexible pyridyl-substituted NHC scaffolds also led to locating two metals in distal positions to lose intermetallic interactions, a) C. E. Strasser, V. J. Catalano, *J. Am. Chem. Soc.* **2010**, *132*, 10009–10011; b) J. Wimberg, S. Meyer, S. Dechert, F. Meyer, *Organometallics* **2012**, *31*, 5025–5033; c) K. Chen, M. M. Nenzel, T. M. Brown, V. J. Catalano, *Inorg. Chem.* **2015**, *54*, 6900–6909; d) T. Simler, K. Müller, T. J. Feuerstein, M. T. Gamer, S. Lebedkin, M. M. Kappes, P. W. Roesky, *Organometallics* **2019**, *38*, 3649–3661.

[11] An imidazo[5,1-*a*]phthalazine-2-ylidene palladium complex was reported as a related NHC-complex, whereas it was not applied to the synthesis of heterobimetallic complexes, K. G. Kishore, O. Ghashghaei, C. Estarellas, M. M. Mestre, C. Monturiol, N. Kielland, J. M. Kelly, A. F. Francisco, S. Jayawardhana, D. Muñoz-Torrero, B. Pérez, F. J. Luque, R. Gámez-Montaño, R. Lavilla, *Angew. Chem., Int. Ed.* **2016**, *55*, 8994–8998.

[12] The reaction conditions were optimized from reported procedure, C. Liu, M. G. Yang, Z. Xiao, L. Chen, R. M. Moslin, J. S. Tokarski, D. S. Weinstein, SULFONE PYRIDINE ALKYL AMIDE-SUBSTITUTED HETEROARYL COMPOUNDS, US2019152948A1, **2019**.

[13] J. T. Hutt, Z. D. Aron, *Org. Lett.* **2011**, *13*, 5256–5259.

[14] A. Collado, A. Gómez-Suárez, A. R. Martin, A. M. Z. Slawin, S. P. Nolan, *Chem. Commun.* **2013**, *49*, 5541−5543.

[15] P. de Frémont, N. M. Scott, E. D. Stevens, S. P. Nolan, *Organometallics* **2005**, *24*, 2411−2418.

[16] Deposition Numbers <url href="https://www.ccdc.cam.ac.uk/services/structures?id=doi:10.1002/chem.202301673"> 2247782 (for **1**), 2247783 (for **1-Cu^{I}Cl**), 2247784 (for **1-Cu^{I}**), 2247785 (for **1-Cu^{II}**), 2247786 (for **1-Ni^{II}**), 2247787 (for **1-Co^{II}Cl**), 2247788 (for **9**), and 2247789 (for **10**)</url> contain the supplementary crystallographic data for this paper. These data are provided free of charge by the joint Cambridge Crystallographic Data Centre and Fachinformationszentrum Karlsruhe <url href="http://www.ccdc.cam.ac.uk/structures">Access Structures service</url>.

[17] Bondi van der Waals radii were applied for the calculations; A. Bondi, *J. Phys. Chem*. **1964**, *68*, 441–451.

[18] M. J. Calhorda, C. Ceamanos, O. Crespo, M. C. Gimeno, A. Laguna, C. Larraz, P. D. Vaz, M. D. Villacampa, *Inorg. Chem*. **2010**, *49*, 8255−8269.

[19] V. J. Catalano, J. M. López-de-Luzuriage, M. Monge, M. E. Olmos, D. Pascual, *Dalton. Trans.* **2014**, *43*, 16486–16497.

[20] E. Hobbollahi, M. List, B. Hupp, F. Mohr, R. J. F. Berger, A. Steffen, U. Monkowius, *Dalton. Trans*. **2017**, *46*, 3438–3442.

[21] a) M. I. Arriortua, T. Rojo, J. M. Amigo, G. Germain, J. P. Declercq, *Acta. Cryst.* **1982**, *B38*, 1323–1324; b) J. Karges, K. Xiong, O, Blacque, H. Chao, G. Gasser, *Inorganica Chim. Acta.* **2021**, *516*, 120137.

[22] a) M. Barley, E. C. Constable, S. A. Corr, R. C. S. McQueen, J. C. Nutkins, M. D. Ward, M. G. B. Drew, *J. Chem. Soc., Dalton. Trans.* **1988**, 2655–2662; b) C. Piguet, G. Bernardinelli, A. F. Williams, *Inorg. Chem.* **1989**, *28*, 2920–2925; A copper(I) acetonitrile complex bearing a terpyridine derivative as a *N*,*N*,*N*-tridentate ligand was reported, in which the four-coordinated complex adopted a highly distorted square-planar geometry, c) V. Madhu, Y. Diskin-Posner, R. Neumann, *Eur. J. Inorg. Chem.* **2011**, 1792–1796.

[23] Bondi van der Waals radius for cobalt has not been reported. Hence, the calculated van der Waals radius (Co: 1.64 Å) was applied, in which the sum of van der Waals radii of Au and Co is estimated as 3.30 Å. The actual distances of Co–Au for **1-Co^{II}Cl** were shorter than the sum of van der Waals radii; S. S. Batsanov, *Inorg. Mater.* **2001**, *37*, 871–885.

[24] Gaussian 16, Revision C.01, M. J. Frisch, G. W. Trucks, H. B. Schlegel, G. E. Scuseria, M. A. Robb, J. R. Cheeseman, G. Scalmani, V. Barone, G. A. Petersson, H. Nakatsuji, X. Li, M. Caricato, A. V. Marenich, J. Bloino, B. G. Janesko, R. Gomperts, B. Mennucci, H. P. Hratchian, J. V. Ortiz, A. F. Izmaylov, J. L. Sonnenberg, D. Williams-Young, F. Ding, F. Lipparini, F. Egidi, J. Goings, B. Peng, A. Petrone, T. Henderson, D. Ranasinghe, V. G. Zakrzewski, J. Gao, N. Rega, G. Zheng, W. Liang, M. Hada, M. Ehara, K. Toyota, R. Fukuda, J. Hasegawa, M. Ishida, T. Nakajima, Y. Honda, O. Kitao, H. Nakai, T. Vreven, K. Throssell, J. A. Montgomery, Jr., J. E. Peralta, F. Ogliaro, M. J. Bearpark, J. J. Heyd, E. N. Brothers, K. N. Kudin, V. N. Staroverov, T. A. Keith, R. Kobayashi, J. Normand, K. Raghavachari, A. P. Rendell, J. C. Burant, S. S. Iyengar, J. Tomasi, M. Cossi, J. M. Millam, M. Klene, C. Adamo, R. Cammi, J. W. Ochterski, R. L. Martin, K. Morokuma, O. Farkas, J. B. Foresman, and D. J. Fox, Gaussian, Inc., Wallingford CT, **2016**.

[25] a) R. F. W. Bader, *Acc. Chem. Res.* **1985**, *18*, 9–15; b) R. F. W. Bader, *Chem. Rev*. **1991**, *91*, 893–928.

[26] Multiwfn program ver. 3.8 for Windows was downloaded from the following website (http://sobereva.com/multiwfn/).; T. Lu, F. Chen, *J. Compute. Chem*. **2012**, *33*, 580–592.
[27] 3D models were described by VMD program ver. 1.9.4a53. W. Humphrey; A. Dalke, K. Schulten, *J. Mol. Graphics* **1996**, *14*, 33.
[28] A. D. Becke, K. E. Edgecombe, *J. Chem. Phys*. **1990**, *92*, 5397–5403.
[29] T. Lu, Q. Chen, *J. Comput. Chem*. **2022**, *43*, 539–555.
[30] J. Österlöf, *Acta. Chem. Scand.* **1950**, *4*, 374–385.
[31] G. M. Sheldrick, *Acta Cryst.* **2015**, *A71*, 3–8.
[32] G. M. Sheldrick, *Acta Cryst.* **2015**, *C71*, 3–8.
[33] V. Dolomanov, L. J. Bourhis, R. J. Gildea, J. A. K. Howard, H. Puschmann, *J. Appl. Crystallogr.* **2009**, *42*, 339–341
[34] L. J. Farrugia, *J. Appl. Crystallogr.* **1997**, *30*, 565.

Entry for the Table of Contents

***Au*,*N*,*N*-tridentate ligand**

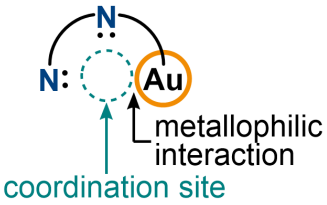

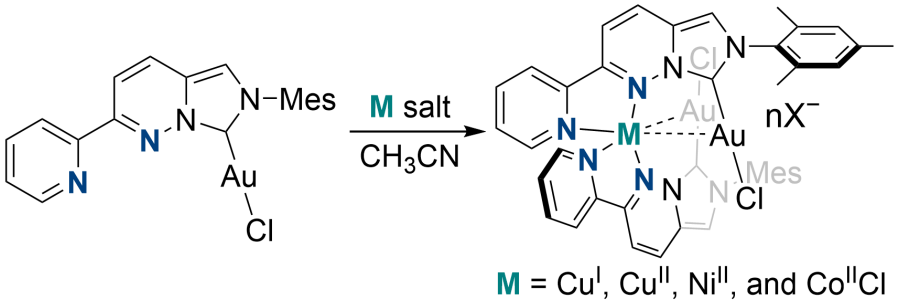

2-(Pyridin-2-yl)imidazo[1,5-*b*]pyridazine-7-ylidene was introduced as a dimetal-binding rigid scaffold. The scaffold was first converted into an *Au*,*N*,*N*-tridentate ligand through binding of Au(I)Cl at the carbene site. By using the *Au*,*N*,*N*-tridentate ligand, various trinuclear heterobimetallic complexes with intermetallic interactions were readily preparable with 3*d*-transition metals (Cu^{I}, Cu^{II}, Ni^{II}, and Co^{II}). The structures of these complexes were unambiguously determined by SC-XRD analysis.